Volume 331, number 1,2, 43–48 FEBS 13002 September 1993

Replacement of His^{23} by Cys in a zinc finger of HIV-1 NC_p7 led to a change in ^1H NMR-derived 3D structure and to a loss of biological activity

N. Julian[a], H. Demene[a], N. Morellet[a], B. Maigret[b], B.P. Roques[a,*]

[a]*Département de Pharmacochimie Moléculaire et Structurale, U266 INSERM-URA D1500 CNRS, Faculté de Pharmacie, 4 ave de l'Observatoire, 75270 Paris, France*
[b]*Université Nancy I, Laboratoire Chimie Théorique, B.P. 239, 54506 Vandoeuvre-lés-Nancy Cédex, France*

Received 5 July 1993

The nucleocapsid protein NCp7 of human immunodeficiency virus type 1 (HIV-1), which is necessary for the formation of infectious virions, contains two zinc fingers of the Cys-X_2-Cys-X_4-His-X_4-Cys form. To elucidate the importance of this particular motif, well conserved in retroviruses and retroelements, we substituted the histidine residue by a cysteine in the first zinc binding domain ^{13}VKCFNCGKEGHTARNCRA^{30}. The structures of the mutated and native zinc complexed peptides were studied by two-dimensional 600 MHz ^1H nuclear magnetic resonance (NMR) in aqueous solution. The nuclear Overhauser effects were used as constraints to determine the solution structures using DIANA software followed by AMBER energy refinement. The results show that native and mutant peptides fold into non-identical three-dimensional structures, probably accounting for the loss of retrovirus infectivity following the His-Cys point mutation.

HIV-1; Nucleocapsid NCp7; Mutagenesis; Peptide structure

1. INTRODUCTION

All retroviruses encode a polyprotein, the Gag precursor, which is ultimately processed into several structural proteins of the mature viral particle. Among them is the nucleocapsid (NC) protein [1,2] which is a low molecular weight, basic, single-stranded nucleic acid binding protein. NC proteins were shown to be involved in retroviral RNA dimerization [3,4] and encapsidation [5–8], as well as in the activation of the primer tRNA annealing to the initiation site for reverse transcription on the viral genome [9,10]. In addition, NC proteins protect the retroviral genome from nucleases in a histone-like manner [11,12]. Therefore, NC proteins represent an interesting target for the development of selective antiviral agents [13,14]. All NC proteins contain one or two copies of a Cys-X_2-Cys-X_4-His-X_4-Cys sequence (CCHX box) suggesting that this motif is essential for the functions of these proteins in the retroviral life cycle. The CCHC boxes were shown to function as zinc binding domains [15], as previously observed for zinc fingers of related DNA-binding proteins [1]. This hypothesis was supported by the demonstration that the zinc atom is tightly bound to NC protein in HIV1 and HTLV1 viruses [16,17], and that the two CCHC domains of HIV-1 NCp7 fold in a stable conformation, induced by the zinc binding [18–21].

*Corresponding author. Fax: (33) 4326 6918.

A series of point mutations in the HIV-1 CCHC box, which affected the zinc binding caused genomic RNA packaging defect [5,7,22] and led to a loss of virion infectivity in the case of the first CCHC box of Rous Sarcoma Virus (RSV) NC protein [8]. These results suggest that the three-dimensional structure of the zinc fingers plays a critical role in the function of NC proteins, accounting for the conservation of the Cys-X_2-Cys-X_4-His-X_4-Cys motif in retroviruses [1,2]. To investigate this hypothesis and with the aim of using the zinc finger motif to design anti-HIV peptidomimetics, we synthesized a mutant of the N-terminal CCHC box of HIV-1 NCp7 in which the histidine residue was replaced by a cysteine (Fig. 1). We report here the ^1H NMR derived three-dimensional solution structure of the (13–30) $H^{23}C$ mutant and the differences with the wild type zinc finger structure.

2. MATERIALS AND METHODS

2.1. *Material and NMR sample preparation*

In order to carry out NMR experiments, large quantities of native and mutant (13–30) NCp7 were synthesized using the stepwise solid-phase method and Fmoc amino-acids on an automatic reprogrammed Applied Biosystem 431A synthesizer, as already described [23].

NMR samples were prepared by dissolving 9.4 mg of mutant (13–30) NCp7 and 9.2 mg of native (13–30) NCp7 in 90% H_2O/10% D_2O and/or 100% D_2O, in the presence of 1.5 equivalents of zinc chloride. The pH was adjusted to 5.7 with small aliquots of 1 M NaOD or 1 M DCl.

2.2. *NMR experiments*

All experiments were carried out on a Bruker AMX 600 spectrometer operating at 600 MHz for protons, with the carrier frequency set on the water resonance. All 2D NMR spectra were acquired in the phase sensitive mode using the time proportional phase increments method. Water peak suppression was achieved by irradiation of the solvent resonance during the relaxation delay and during the mixing time for the NOESY spectra. For most experiments, 512 t_1 values were usually acquired with either 64 or 128 scans per t_1 increment. Double quantum filtered COSY (DQF-COSY) spectra [24] were obtained using the standard pulse sequence and phase cycling. Phase-sensitive NOESY spectra [25,26] were assessed using standard methods with 100 and 200 ms mixing periods. TOCSY experiments [27,28] were performed with a total mixing time of 55 ms. For the mutant (13–30), spectra recorded at 20° and 30° allowed to resolve the ambiguities arising from degeneracies of some resonances

2.3. *NMR derived constraints*

For the mutant (13–30) NCp7, most NOEs were observed using 200 ms and 100 ms mixing times NOESY spectra. Some weak NOEs, present only at a mixing time of 200 ms, were considered only when no spin diffusion pathway was evident [29]. NOEs intensities were calibrated on the basis of the relative amplitude of the cysteine geminal protons, used as an internal standard

2.4. *Structure calculations*

The inter proton distance constraints were classified into three categories: 2.0–2.5, 2.0–3.5 and 2.0–4.5 Å corresponding to strong, medium and weak NOEs respectively. The DIANA distance geometry package [30] was used with the protocol already described by Morellet and co-workers [18]. A total of 50 structures were generated and the ten best, based on an arbitral final error function cut off, were refined by energy minimization using the AMBER package [31]. A zinc force field, obtained from ab-initio calculations and parameterized in the AMBER framework, was used in the refinement procedures to account for zinc ion/peptide interactions. Moreover a dielectric constant of 80 was used to minimize ion pair interactions overestimated in in vacuo calculations. Computer graphic representations were obtained using the INSIGHT molecular modelling package (BIOSYM Technologies Inc., San Diego, CA) on a Personal IRIS 4D35 workstation (Silicon Graphics Inc.). All structural calculations were performed on a RISC System/6000-550 workstation (IBM).

3. RESULTS AND DISCUSSION

3.1. *NMR experiments*

The 1D ^{1}H NMR spectra of mutant and native (13–30) NCp7 in the presence of zinc display the wide chemical shift dispersion characteristic of folded conformations (not shown). Moreover, in both cases, the observation of a single set of resonances indicates the presence of a unique species in solution.

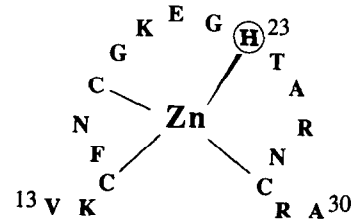

Fig. 1. Primary structure of the (13–30) zinc finger domain of HIV-1 NCp7. The site of point mutation is circled.

3.2. *Sequential resonance assignment*

The ^{1}H chemical shifts of the native zinc finger studied here were closely related to those reported for the corresponding protons in the entire NCp7 [17,18]. The different spin systems were firstly identified using the D_2O and H_2O DQF COSY spectra, as well as the H_2O TOCSY spectra. Sequence specific assignments were carried out by standard methods. The chemical shifts for the mutant and native (13–30) NCp7 are listed in Table I. In this 18 amino acid peptide, 17 dαN sequential connectivities were expected. Of these, all but those of α18 and NH19 (due to partial saturation of the α resonance situated at 4.83 ppm) and of α17 and NH18, were observed. In that particular case, sequential assignment was achieved thanks to the NOE connectivities between the NH protons and the β ones of the preceding residue. The NOESY spectra (mixing time of 100 ms) showing the amide to alpha protons connectivities of native and mutant (13–30) NCp7 are depicted in Fig. 2A and 2B, respectively.

These spectra show the chemical shift dispersion of the NH and α resonances as well as the significant differences between native and mutant peptides. Interestingly, the chemical shift variations between both peptides are not only observed at the mutation level but occurred also all along the peptide chain. In fact, the NOESY spectrum of native (13–30) NCp7 exhibits the characteristic cross peaks of retroviral type zinc finger:

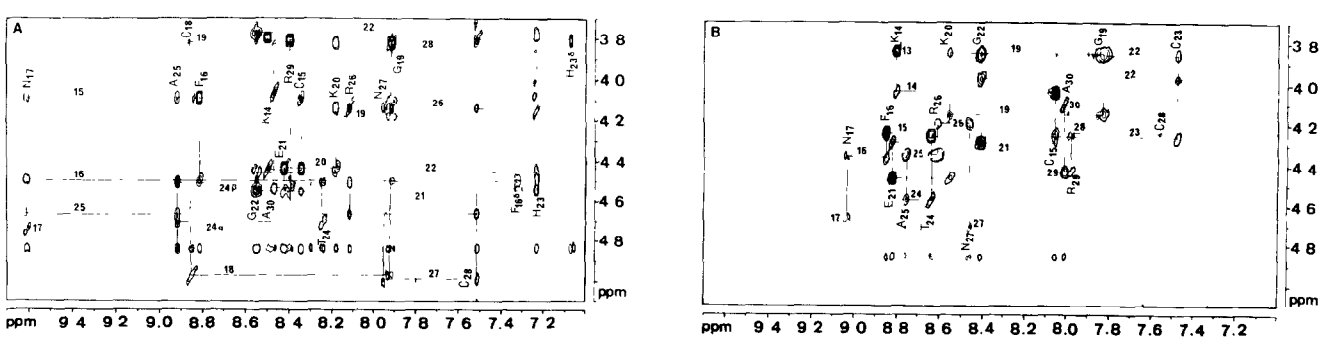

Fig. 2. Portion of the NOESY spectra recorded for native (13–30) NCp7 (A) and for mutant (13–30) NCp7 (B) in H_2O at pH 5.7 and 20°C with a mixing time of 100ms, showing connectivities between NH and aH resonances.

sequential amide to amide cross peaks from Phe[16] to Lys[20] and from Ala[25] to Cys[28], the pattern of CβH(15)/NH18,19,20 connectivities and the numerous connectivities from the imidazole ring protons (Cδ2H and Cε1H) of His[23] to residues Lys[20], Asn[27] and Cys[28]. For the mutant (13–30) NCp7, we found a stretch of NH-NH connectivities from Phe[16] to Lys[20] and from Asn[27] to Arg[29]. Numerous long range NOEs present in NOESY spectra of native (13–30) NCp7 were not observed in the corresponding NOESY spectra for the mutant peptide. In particular, the NOEs between the aromatic H_{2-6} protons of Phe[16] and the β protons of Ala[25] which were also observed in the NOESY spectra of the whole protein (Morellet et al., in press), are no longer present for the mutant (13–30) NCP7. On the other hand, some medium NOEs were only observed in the case of the mutant peptide. This is the case of the β protons of Lys[14] and the α protons of Gly[19], and the β protons of Asn[17] and the a proton of Cys[28]. Fig. 3 displays the diagonal plot representation of NOEs for the mutant peptide (below the diagonal) and for the native peptide (above the diagonal). The differences evidenced in the NOEs diagonal plot (Fig. 3) and in the backbone chemical shifts (Fig. 4) provide strong evidence that the two peptides fold into two different conformations.

At pH 8, the remaining amide resonances for mutant (13–30) NCp7 are those of residues 15, 17, 19, 20, 23, 28, 29 and 30 and for the native peptide those of residues 17, 19, 20, 23, 28 and 30. For both peptides, the resonances of the Hd of residue Asn[17] were observed.

3.3. *Structure description*

(i) Wild-type CCHC zinc finger. Distance geometry calculations using DIANA were performed with a total of

Table I

^{1}H chemical shifts, δ (ppm) for mutant (13–30) NCp7 and native (13–30) NCp7 at pH 5.7 and 20°C[a]

Residue	NH	CαH	CβH	Others
Val[13]	–[b]	3.84 (3.79)	2.18 (2.04)	γCH$_3$ 0.99, 0.85 (1.03)
Lys[14]	8.79 (8 47)	4 04 (4.43)	1.61 (1.53)	γCH$_2$ 1.01 (1.36)
	1.19		1.48 (1.45)	δCH$_2$ 1.20 (1 64)
				εCH$_2$ 1.87 (3.00)
Cys[15]	8.02 (8.33)	4.25 (4.09)	3.33 (2.78, 1.77)	
Phe[16]	8.83 (8.79)	4.37 (4.49)	3.23 (3.23)	2,6H 7.33 (7.32)
			3 15 (3.16)	3.5H 7.39 (7.39)
				4H 7.39 (7.40)
Asn[17]	9.03 (9.60)	4.67 (4.74)	2.76 (3.16)	δNH$_2$ (8.05) 8.28
			2.53 (2.77)	7.04 (7.00)
Cys[18]	8.42 (8.84)	4.830 (4.70)	3.20 (3.26)	
			2.83 (2.57)	
Gly[19]	7.79 (7.90)	4.15 (4.17)		
		3.86 (3.82)		
Lys[20]	8.55 (8.17)	4.47 (4.43)	1.96 (1 89)	γCH$_2$ 1.62 (1.62)
				1 49 (1.49)
			1.80 (1.83)	δCH$_2$ 1.73 (1.72)
				εCH$_2$ 3.05 (3 05)
Glu[21]	8 81 (8.40)	4.29 (4.51)	1.93 (1.93, 1.88)	γCH$_2$ 2.22 (2.28)
				2.19 (2.16)
Gly[22]	8.38 (8.52)	3.97 (4.49)		
		3.86 (3.77)		
Cys[23]	7.47	4.26[c]	3.03 (3.22)	
His[23]				2H 2.74; 4H 7.06
Thr[24]	8.62 (8.22)	4.57 (4.69)	4.57 (4 49)	δCH$_3$ 1.18 (1.19)
Ala[25]	8.78 (8.92)	4.34 (4.65)	1.48 (1.47)	
Arg[26]	8.60 (8.10)	4.20 (4.13)	1.84 (1.83, 1.73)	γCH$_2$ 1.63 (1.71); 1.67
				δCH$_2$ 3.20 (3.24)
				NH 7.20 (7 23)
Asn[27]	8.45 (7.94)	4.71 (4.98)	2.81 (3.02, 26.1)	γNH$_2$ 7.75 (7.63)
				6.89 (6 91)
Cys[28]	7.54 (7.50)	4.25 (3 77)	2.92 (3.34)	
			2.86 (2.99)	
Arg[29]	7 94 (8.36)	4.43 (4.48)	1.96 (1.97)	γCH$_2$ 3.13 (3.19)
				1.57 (1.77)
				δCH$_2$ 3.13 (3.19)
				NH 7.20 (7.12)
Ala[30]	7.98 (8.43)	4.10 (4.05)	1.34 (1.31)	

[a] Chemical shifts measured relative to internal H_2O (4.828 ppm).
[b] Signal for terminal NH_3^+ not observed.
[c] Signal for αH could not be assigned because of bleaching out by water resonance saturation.

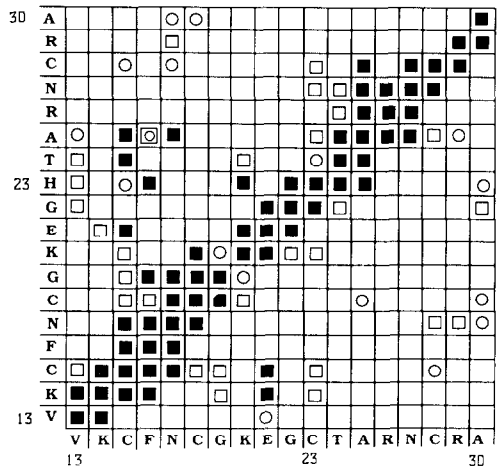

Fig. 3. Noe pattern of native (13–30) NCp7 (above the diagonal) and mutant Cys[23](13–30) NCp7 (below the diagonal). Solid boxes denote NOES between backbone protons, open boxes NOES between side chain and backbone protons, open circles between side chain protons.

202 relevant distance constraints distributed into 20 intra residual and 182 inter residual upper limits. The distribution of the inter residual constraints was as follows: 69 were sequential ($i,i+1$), 51 were medium range ($i,i+2 \leq j \leq i+4$), and 62 were long range interactions ($i,j \geq i+5$). The ten structures generated through DIANA calculations were further minimized using AMBER. For clarity, Fig. 5a shows a superimposition of the 6 best conformations obtained after best fit of the (15–28) backbone atoms: the root mean square deviation (rmsd) is about 1.059 ± 0.044 Å. The final total energy is 78.3 ± t1.6 kcal/mol.

The Cys[15]–Cys[18] fragment forms a type VII β-turn characterized by the dihedral angle values of Phe[16] ($\phi = -97 \pm 62$, $\psi = 39 \pm 9$) and Asn[17] ($\phi = -164 \pm 2$, $\psi = -75 \pm 5$).The Gly[22]–Ala[25] residues are involved in a type X β-turn with the dihedral angle values of His[23] being $\phi = -79 \pm 4$, $\psi = 79 \pm 79$ and Thr[24], $\phi = 17 \pm 74$, $\psi = -83 \pm 17$. A type I β turn is observed for residues Ala[25]–Cys[28] with the following dihedral angle values for Arg[26] ($\phi = -71 \pm 24$, $\psi = 35 \pm 22$) and Asn[27] $\phi = -85 \pm 20$, ψ 60 ± 28).

(ii) Mutant CCCC zinc finger. DIANA calculations were performed as described for the native peptide (see above) with a total of 237 relevant distance constraints, including 91 intra residues. The remaining 146 inter residual upper limits were distributed as follows: 73 were sequential (i, $i+1$), 28 were medium range (i, $i+\leq j \leq i+4$), and 45 were long range interactions ($i,j \geq i+5$). Fig. 5b shows a superimposition of the 6 best conformations obtained after best fit of the (15–28) backbone atoms: the root mean square deviation is about 0.983 ± 0.168 Å. The final total energy is 82.8 ± 1.7 kcal/mol.

The Cys[15]–Cys[18] fragment is involved in a type III β turn conformation, characterized by the dihedral angle values of Phe[16] ($\phi = -67 \pm 7$, $\psi = -27 \pm 8$) and Asn[17] ($\phi = -56 \pm 4$, $\psi = -51 \pm 7$), and stabilized by a tight hydrogen bond between the Cys[15] carbonyl oxygen and the Cys[18] amide proton. The Lys[20]–Cys[23] residues are involved in a type III β-turn conformation with the following dihedral angle values for Glu[21] ($\phi = -87 \pm 16$, $\psi = -15 \pm 24$) and Gly[22] ($\phi = -68 \pm 11$, $\psi = -87 \pm 12$).

3.4. *Comparison of native and mutant zinc finger*

To assess the contribution of the histidine mutation to the chemical shift variations, the local effects of the histidine ring current on the chemical shifts of spatially close protons were estimated from the NMR-derived structure of the native zinc finger. However, the α proton of Thr[24], the NH of Arg[29] whose resonances were expected to be upfield shifted following the replacement of His[23] by Cys were found at lower fields (+0.12 and 0.42 respectively). This chemical shift variation between both peptides confirms the NMR-derived structure evidencing a spatial rearrangement of the mutant zinc finger.

The superimposition of the mutant CCCC zinc finger onto the CCHC native one showed rmsd values of around 2.902 ± 0.030 Å when all the backbone atoms were considered between Cys[15] and Cys[28]. When the backbone atoms of residues Cys[15] to Gly[22] were superimposed, the rmsd decreased to 1.413 ± 0.022 Å (Fig. 6). As already suggested by the NOE patterns (Fig. 3), the global folding of the (15–22) segment are similar for both native and mutant peptides (Fig. 6). Thus, particu-

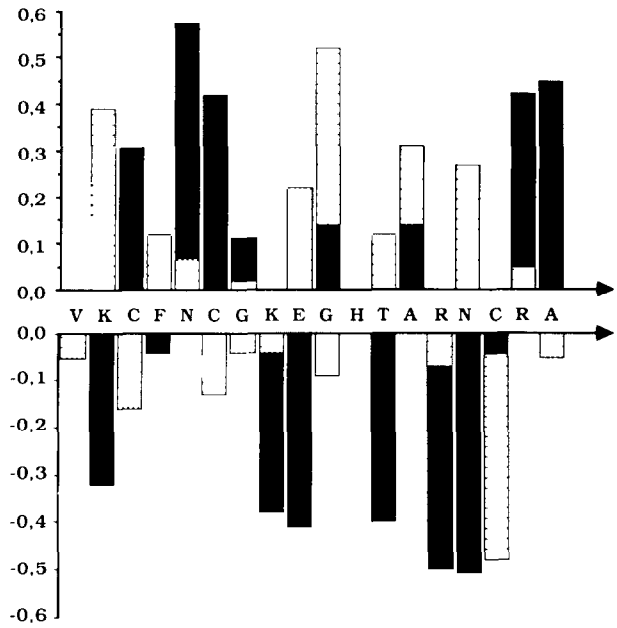

Fig. 4. Plot of the differences of the chemical shifts of the NH (black boxes) and α protons (hatched boxes) between native (13–30) NCp7 and mutant Cys[23](13–30) NCp7.

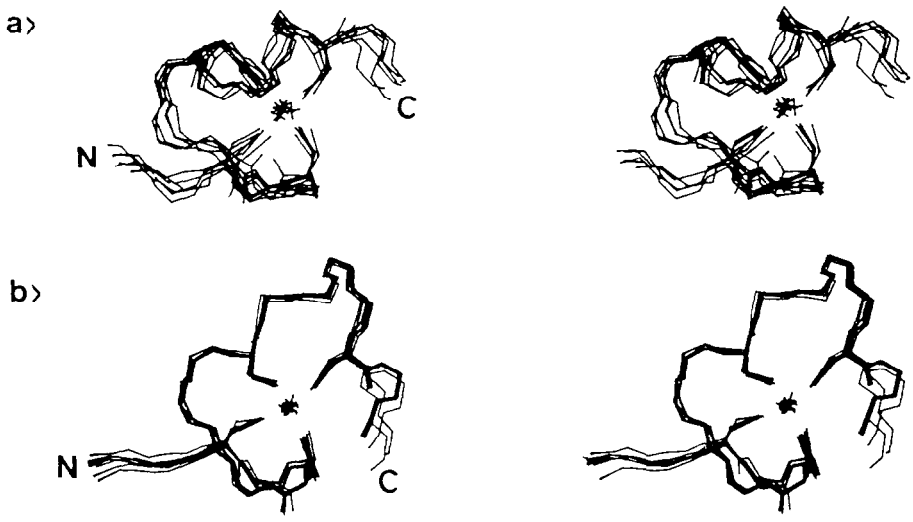

Fig. 5. Stereo view of the backbone atoms of: (a) the native and (b) the mutant zinc finger: the same orientation is respected for residues from V^{13} to G^{22}.

lar attention was paid to the (23–28) region in order to characterize the structural differences between the two zinc fingers. The $His^{23} \rightarrow Cys$ mutation introduces a local distortion in the polypeptide backbone at the level of the (23–28) segment, characterized by the rmsd values of 2.437 ± 0.037 Å. A tight hydrogen bond involving the carbonyl oxygen of Thr^{24} and the amide hydrogen of Arg^{26} was only observed for the mutant peptide (Fig. 6).

It is of interest to note that all four cysteine zinc fingers reported to date bird zinc through a tetrahedral geometry [32–34]. This structural requirement probably accounts for the different polypeptide chain folding observed for the wild-type and the mutant zinc fingers. The $^{23}His \rightarrow Cys$ mutation occurring in a sequence preceding the short spacer, linking together the two zinc fingers of NCp7, will change the spatial orientation of this latter.

It is noteworthy that the three-dimensional structure of the (1–72) NCp7 is characterized by a particular orientation of one zinc finger relative to the other, resulting in the spatial proximity of Phe^{16} and Trp^{37} aromatic residues [18]. This biologically relevant folding is favoured by a Pro^{31} residue located in the short sequence ^{29}RAPRKKG linking together the two zinc fingers. Thus, a synthetic NCp7 with a D-Pro^{31} residue was shown to loss its annealing activities in vitro in agreement with a disapearence of the spatial interactions between Phe^{16} and Trp^{37} observed by NMR spectroscopy (Morellet et al., in press). Moreover, this spatial proximity is important for in vivo infectivity, since replacement of the Pro^{31} residue by a leucine led to non-infectious viral particles (Morellet et al., in press).

4. CONCLUSION

Complete ^{1}H resonance assignments of wild-type and mutant C^{23} zinc fingers have been determined by two-dimensional NMR spectroscopy. Both zinc fingers adopt different three-dimensional structures in the pres-

Fig. 6: Superimposition of α carbon chain of residues from V^{13} to G^{22}: the arrow indicates the site of point mutation. From the arrow, the top ribbon corresponds to the mutant Cys^{23} (13–30) NCp7.

ence of zinc, as illustrated by the variations of proton chemical shifts. The structural differences occur in the polypeptide backbone corresponding to the segment ^{23}CTARNC^{28} which follows the site of point mutation and precedes the linker sequence ^{29}RAPRKKG^{35} in the entire NCp7. This is expected to induce a change in the mutual orientation of the two zinc fingers. Experiments are currently in progress to determine the three dimensional structure of the mutant H^{23}C (1–72) NCp7, but preliminary biological tests seem to indicate a loss of activity following mutation of this well conserved zinc coordinating residue.

Acknowledgements D. Ficheux is acknowledged for his contribution in the peptides synthesis. The authors thank A Beaumont and N Goudreau for stylistic revision of the manuscript and C Dupuis for her assistance in preparing it. This work was supported by the Association Nationale de Recherche sur le SIDA and the Institut de Formation Supérieure Biomédicale

REFERENCES

[1] Berg, J.M. (1986) Science 232, 485–487.
[2] Covey, S.N. (1986) Nucleic Acids Res. 14, 623–632.
[3] Coffin, J.M (1984) in: RNA Tumor Viruses (Weiss, R., Teich, N., Varmus, H. and Coffin, J.M. Eds) Vol. 1, pp. 261–368, Cold Spring Harbor Laboratory Press, New York.
[4] Prats, A.C., Roy, C., Wang, P., Erard, M., Housset, V., Gabus, C., Paoletti, C. and Darlix, J.L (1990) J. Virol. 64, 774–783.
[5] Méric, C. and Spahr, P.F. (1986) J. Virol. 60, 450–459.
[6] Méric, C and Goff, S. (1989) J. Virol. 63, 1558–1568
[7] Aldovini, A. and Young, R.A. (1990) J. Virol. 64, 1920–1926.
[8] Dupraz, P., Oertle, S., Méric, C., Damay, P. and Spahr, P.F. (1990) J. Virol 64, 4978–4987.
[9] Prats, A.C., Sarih, L., Gabus, C., Litvak, S., Keith, G. and Darlix, J.L. (1988) EMBO J. 7, 1777–1783.
[10] Barat, C., Lullien, V., Schatz, O., Keith, G., Nugeyre, M.T., Grüninger-Leitch, F., Barré-Sinoussi, F., Le Grice, S.F.J. and Darlix, J.L. (1989) EMBO J. 8, 3279–3285.
[11] Bowsles, N.E., Damay, P. and Spahr, P.F. (1993) J. Virol 67, 623–631.
[12] Aronoff, R., Hajiar, A.M. and Linial, M.L (1993) J. Virol 67, 178–188
[13] De Rocquigny, H., Gabus, C., Vincent, A., Fournié-Zaluski, M C., Roques, B.P. and Darlix, J.L. (1992) Proc Natl Acad Sci. USA 89, 6572–6476.
[14] Rice, W G., Schaeffer, C.A., Harten, B., Villinger, F., South, T.L., Summers, M.F., Henderson, L.E., Bess, J.W., Arthur, L.O., McDougal, J S., Orloff, S.L., Mendeleyev, J and Kun, E. (1993) Nature 361, 473–475
[15] Mély, Y., Cornille, F., Fournié-Zaluski, M.C., Darlix, J.L., Roques, B.P. and Gérard, D. (1991) Biopolymers 31, 899–906.
[16] Summers, M.F., Henderson, L.E., Chance, M.R., Bess, J.W., South, T L., Blake, P.R., Sagi, I., Perez-Alvarado, G., Sowder III, R.C., Hare, D.R. and Arthur, L.O. (1992) Prot. Sci 1, 563–574.
[17] Bess Jr., J.W., Henderson, L.E., Arthur, L.O., South, T.L., Perez-Alvarados, G and Summers, M.F. (1992) Proc. Natl. Acad. Sci. USA 89, 10041–10045.
[18] Summers, M.F., South, T L., Kim, B. and Hare, D.R. (1990) Biochemistry 29, 329–340.
[19] South, T.L., Blake, P.R., Hare, D.R and Summers, M.F. (1991) Biochemistry 30, 6342–6349.
[20] Omichinski, J.G., Clore, G.M., Sakaguchi, K., Apella, E. and Gronenborn, A.M (1991) FEBS Lett. 292, 25–30.
[21] Morellet, N., Jullian, N., De Rocquigny, H., Maigret, B., Darlix, J.L and Roques, B.P. (1992) EMBO J. 11, 3059–3065.
[22] Gorelick, R.J., Nigida, S.N., Bess, J.W, Arthur, L.O., Henderson, L.E and Rein, A (1990) J. Virol. 64, 3207–3211
[23] De Rocquigny, H., Ficheux, D., Gabus, C., Fournié-Zaluski, M.C., Darlix, J.L and Roques, B.P. (1991) Biochem. Biophys. Res. Commun. 180, 1010–1018.
[24] Rance, M., Sorensen, O.W., Bodenhausen, G., Wagner, G., Erust, R.R and Wuthrich, K. (1983) Biochem. Biophys. Res. Commun. 117, 479–485.
[25] Jeener, J., Meier, B.H., Bachmann, P. and Erust, R R. (1979) J. Med. Chem. Phys. 71, 4546–4553.
[26] Macurra, S., Huang, Y., Suter, D. and Ernst, R.R. (1979) J. Chem. Phys. 71, 4546–4553.
[27] Braunochweiler, L and Erust, R R. (1983) J Magn Reson. 43, 259–291
[28] Davis, D.G and Bax, A (1985) J. Am. Chem. Soc 107, 2821–2822.
[29] Kochoyau, M., Havel, T F., Nguyen, D., Dahl, C.E., Keutman, H.T. and Weiss, M.A. (1991) Biochemistry 30, 3371–3886.
[30] Güntert, P., Braun, W. and Wüthrich, K (1991) J. Mol. Biol. 217, 517–530.
[31] Singh, U.C., Weiner, P.K., Caldwell, J. and Kollman, P.A. (1986) AMBER (UCSF version 4.0) School of Pharmacy, University of California, San Francisco, CA 94143.
[32] Schwabe, J.W R., Neuhaus, D. and Rhodes, D (1990) Nature 348, 458–461.
[33] Freedman, L.P., Luisi, B.F., Korszun, Z.R., Basavappa, R., Sigler, P B. and Yamamoto, K.R. (1988) Nature 334, 543–546.
[34] Härd, T., Kellenbach, E., Boelens, R., Maler, B.A., Dalihlman, K., Freedman, P.L., Carlsteat-Duke, J., Yamamoto, K.R., Gustafsson, J. and Kaptein, R (1990) Science 249, 157–160